Maximizing Quality of Coverage under Connectivity Constraints in Solar-Powered Active Wireless Sensor Networks

BENJAMIN GAUDETTE and VINAY HANUMAIAH, Arizona State University
MARWAN KRUNZ, University of Arizona
SARMA VRUDHULA, Arizona State University

Energy harvesting is a promising solution for reducing network maintenance and the overhead of replacing chemical batteries in sensor networks. In this article, problems related to controlling an active wireless sensor network comprised of nodes powered by both rechargeable batteries and solar energy are investigated. The objective of this control is to maximize the network's Quality of Coverage (QoC), defined as the minimum number of targets that can be covered by the network over a 24-hour period. Assuming a time-varying solar profile, the underlying problem is to optimally control the sensing range of each sensor so as to maximize the QoC. The problem is further constrained by requiring all active sensors to report any sensed data to a centralized base station, making connectivity a key factor in sensor management. Implicit in the solution is the allocation of solar energy during the day to sensing tasks and recharging of the battery so that a minimum coverage is guaranteed at all times. The problem turns out to be a nonlinear optimal control problem of high complexity. By exploiting the particular structure of the problem, we present a novel method for determining near-optimal sensing radii and routing paths as a series of quasiconvex (unimodal) optimization problems. The runtime of the proposed solution is 60X less than the standard optimal control method based on dynamic programming, while the worst-case error is less than 8%. The proposed method is scalable to large networks consisting of hundreds of sensors and targets. Several insights in the design of energy-harvesting networks are provided.

Categories and Subject Descriptors: C.2.4 [**Computer-Communication Networks**]: Distributed Systems–*Distributed applications*; G.1.6 [**Numerical Analysis**]: Optimizations–*Constrained optimization, gradient methods*

General Terms: Algorithms, Design, Performance

Additional Key Words and Phrases: Active sensor networks, network coverage, network connectivity, energy harvesting, quasiconvex optimization, min-flow

ACM Reference Format:
Benjamin Gaudette, Vinay Hanumaiah, Marwan Krunz, and Sarma Vrudhula. 2014. Maximizing quality of coverage under connectivity constraints in solar-powered active wireless sensor networks. ACM Trans. Sensor Netw. 10, 4, Article 59 (April 2014), 27 pages.
DOI: http://dx.doi.org/10.1145/2594792

Portions of this work appeared in preliminary form in Gaudette et al. [2012].
V. Hanumaiah is now with Samsung Information Systems America, San Jose, CA 95134.
This research was supported in part by NSF under grants CNS-0904681 and IIP-0832238, and by a grant from the Science Foundation Arizona and Stardust Foundation. Any opinions, findings, conclusions, or recommendations expressed in this paper are those of the author(s) and do not necessarily reflect the views of the sponsors.
Authors' addresses: B. Gaudette (corrrsponding author) and V. Hanumaiah, Department of Computer Science and Engineering, Arizona State University, Tempe, AZ 85281; email: bgaudett@asu.edu; M. Krunz, Department of Electrical and Computer Engineering, University of Arizona, Tucson, AZ 85721; S. Vrudhula, Department of Computer Science and Engineering, Arizona State University, Tempe, AZ 85281.

DOI: http://dx.doi.org/10.1145/2594792

1. INTRODUCTION

A wireless sensor network (WSN) consists of many sensor nodes that are spatially distributed over some geographical area. The feasibility of such large networks is attributed to advances in microelectronics, which allow for low-cost and low-power circuitry to be implemented in sensor nodes. In the case of active sensor networks, sensors must spend energy to monitor various targets. This makes the task of managing the network's energy supply and consumption a vital part of ensuring high network performance.

Adding to the benefit of low cost is the versatility of sensor networks. Modern sensor networks typically do not to require a preexisting infrastructure, such as power lines or network cables, but instead use chemical batteries for sensing, and radio-frequency integrated circuits (RF IC) for communications. This flexibility comes with a number of challenges with regard to the management of such a network. As a result, a substantial body of research has been conducted on power management for WSNs at the physical, networking, and application layers [Akyildiz et al. 2002]. Regardless of their energy efficiency, battery-powered WSNs will eventually cause the network to fail due to their limited power supply, or their batteries will need to be replaced. This can be a costly procedure if the network is deployed in a harsh environment or in an inaccessible location. A promising solution to this problem is the use energy harvesting in conjunction with batteries. In this article we consider solar-energy harvesting.

Photovoltaic panels (solar panels) are becoming relatively inexpensive to manufacture and very efficient [Torcellini et al. 2006]. However, proper utilization of energy harvesting can be burdensome and complex. The unpredictable nature of the solar profile (cloud cover, shadows of buildings, etc.) introduces a high degree of uncertainty and difficulty in the management of sensors (adjusting their radii, sampling intervals, etc.). Consequently, the basic problem of guaranteeing a minimum coverage of targets becomes more acute with energy harvesting. The importance of this objective over other similar objectives (e.g., maximizing average coverage) stems from a very important application of active sensor networks, namely surveillance. In surveillance networks, periods of low coverage represent times of vulnerability to outside influences. As such, it is important to eliminate these periods by ensuring that the minimum coverage experienced throughout the operational time is maximized.

This article offers a novel procedure to utilize the abundant source of energy from the Sun in order to maximize the quality of coverage (QoC). More specifically, this article addresses the *target coverage* problem in the context of solar-powered active sensor networks in which each sensor's range is controllable. In this context, QoC is defined as the minimum number of monitored targets at any given time during the period of network operation. Furthermore, the definition of a monitored (also called covered) target is further constrained by the necessary condition that any sensed data must be reported back to the base station (also referred to as the sink). In other words, at any point in time, any active sensor must have a route to the sink. The problem formulation turns out to be a nonlinear optimal control problem, which is, in practice, hard to solve. Using several key observations, a near-optimal solution can be obtained by performing a binary search over the QoC, where each iteration solves a series of quasiconvex optimization problems for all time instants while ensuring that the assumed QoC is met for that iteration. Additionally, the traffic routing constraint is formulated either as a linear program or as an integer linear program, depending on the network and design tolerances. This program is then solved at each iteration to determine the feasibility of the assumed QoC.

Our simulation results indicate a 60X improvement in computation time for the proposed solution over an optimal dynamic programming (DP) solution, with peak error

of 8% in the QoC. The proposed solution is scalable to large networks with hundreds of sensors and targets. The efficiency and the accuracy of the solution method permits exploration of the network design space. In one experiment, the trade-off between the cost of constructing a sensor node and the number of sensor nodes needed to ensure full target coverage is examined. The results suggest that there is a unique optimal number of nodes and corresponding average radii that minimize the network setup cost while guaranteeing a specified QoC. In two other experiments, we find that for certain deployment scenarios, increasing the sampling time of sensors can increase the minimum cover, and increasing the sensor beamwidth has diminishing returns on improving the QoC.

2. RELATED WORK

One of the fundamental problems in sensor networks is the *target cover* problem. An informal yet intuitive description of this problem is given in the Art Gallery Problem [Chvatal 1975]: Given a floorplan of an art gallery, find the minimum number of stationary guards who are needed to monitor every exhibit in the art gallery, assuming that guards have a known field of vision. This problem has been optimally solved in 2D space [O'Rourke 1998].

In sensor networks, sensor nodes ("guards") and targets ("art exhibits") are assumed to have fixed locations at a given time; therefore, a subset of these sensor nodes that collectively covers all targets needs to be determined. When sensors have the same fixed sensing radius, the problem of maximizing the point-cover (where targets are a collection of points in space) can be solved efficiently using binary decision diagrams [Dasika et al. 2006]. The problem of maximizing area coverage can be solved via perimeter analysis using known geometric properties of the disk-based sensing region [Huang and Tseng 2003]. Neither of these approaches considers variable-range sensors.

When considering the limited energy supply of sensor nodes, the cover problem can be stated as a network lifetime maximization problem. The goal of this problem is to prolong the period in which all targets are covered. Several heuristics attempt to achieve this, either by minimizing the total energy consumption [Diamond et al. 2008; Yick et al. 2008] or by prolonging the lifetime of the weakest node [Dasika et al. 2006].

One can further bring the network lifetime problem closer to reality by considering connectivity, thus ensuring all data is sufficiently routed to the sink. A substantial amount of research has been conducted on problems related to the connectivity with battery-powered sensor networks. Liu et al. [2006] consider both the coverage and connectivity problems in WSNs. They provide a randomized scheduling algorithm that assumes probabilistic levels of QoC. Connectivity is then ensured by turning on additional sensor nodes until all nodes are connected to the sink. Zhang and Hou [2004] proposed an alternative solution to the connectivity and coverage problems called Optimal Geographical Density Control (OGDC). They proved that any WSN with full area coverage would be connected if the radio range of the sensors is at least twice that of the sensing range, assuming that all sensors use the same sensing range. Based on this property, they constructed a distributed solution that determines the communication radius for each sensor node. The limitation of this work is the assumption that sensors cannot control their sensing radius. Our work considers control over both the sensing radii and the communication paths between sensor nodes.

In Cardei et al. [2005], the lifetime problem was extended further by introducing multiple discrete sensing ranges. Each sensor may select a different discrete range at any given time. This problem is referred to as the *operational range assignment problem* (ORAP). The authors of Cardei et al. [2005] have shown that the ORAP is NP-complete, and have provided several heuristics and approximations. One approximation is based on a centralized linear programming (LP) approach, which finds a

series of valid covers that maximize the network lifetime. Another approximate solution uses a greedy heuristic, whereby covers are constructed by sequentially increasing a node's sensing radius until the maximum number of targets are covered. The time complexities of these solutions quickly deteriorate as the number of discrete sensing ranges increases. In the present work, continuous control of sensing range is assumed, and the solution provided is shown to be both accurate and computationally efficient.

The solution from Cardei et al. [2005] was extended in Younis et al. [2007] by accounting for uncertainty in the sensor locations. A distributed approach was used to solve the ORAP in a manner similar to the greedy method used in Cardei et al. [2005]. The approach in Younis et al. [2007] consists of two phases. In the first phase, sensors increase their radii in the order of their remaining battery lifetimes until all targets are covered. In the second phase, the radii are decreased while ensuring that full coverage is still met. Although this method increases the network lifetime substantially, it does not incorporate energy harvesting.

In Gaudette et al. [2012], the maximum QoC problem was first formulated in the context of solar-powered sensor networks. A near-optimal solution was presented based on quasiconvex programming. While this solution provided a major first step in solving the radii control problem of solar-powered sensor networks, it lacks a key component, namely, adaptive traffic control. Previously, the network communication overhead was assumed static, which in practice is not practical and is in fact directly dependent on the sensing radii schedules (due to the shared and limited energy resources). In this article we strengthen the previous solution of Gaudette et al. [2012] by modeling message traffic and determining the optimal multihop routing matrix.

There has been some focus on increasing network lifetime through better message routing protocols in solar-powered networks. Niyato et al. [2007] analyzed the unpredictability of energy harvesting via solar radiation. With the use of Markovian models and game theory, sensors establish a scheme for setting the radii, and in doing so, attempt to achieve a balance between two objectives: maximizing battery lifetime and increasing the overall energy efficiency of the network by minimizing the losses in message passing due to poor synchronization between the sender and the receiver.

In Voigt et al. [2004], a set of routing protocols for battery-powered WSNs is introduced, with the goal of avoiding message routing through areas of the network with reduced solar energy. A gradient is formed at each sensor node, which determines the subsequent path of a message leading to the destination. Results show that considerable energy savings are possible by shifting the burden away from resource-limited nodes. Both works only consider the connectivity of the network, and do not consider the underlying task of the network, namely, maximizing the target-cover, as is done in the present work.

3. SYSTEM MODELS

Figure 1 shows the setup of a typical energy-harvesting sensor node. The node consists of: (a) an active sensor (radar, ultrasonic, etc.); (b) a microcontroller unit with memory; (c) an RF communication unit; and (d) an energy-harvesting unit (a small solar panel) with a rechargeable battery and a power management circuitry. The function of the energy management circuitry is to control the charging and discharging of the battery. It is assumed that the solar panel and the battery can simultaneously supply power to the sensor node. Likewise, the solar panel may charge the battery and power the sensor node at the same time.

3.1. Solar Profile

A *solar profile* is the temporal distribution of power provided by the solar panel. The solar profile can be viewed as a random process. However, the theoretical maximum

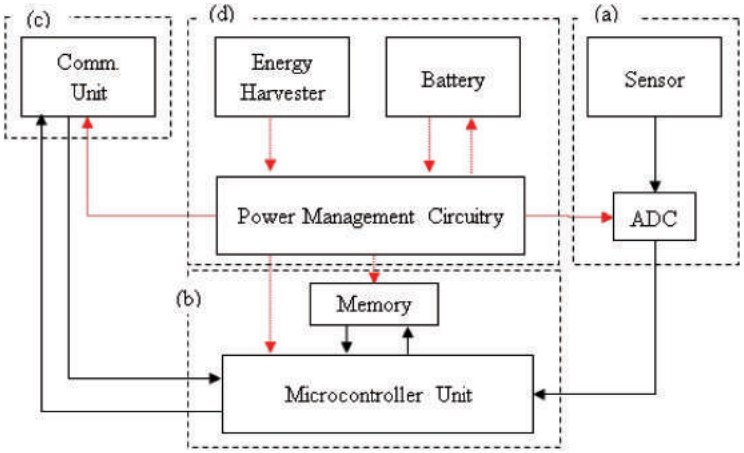

Fig. 1. Architecture of a typical energy-harvesting sensor node.

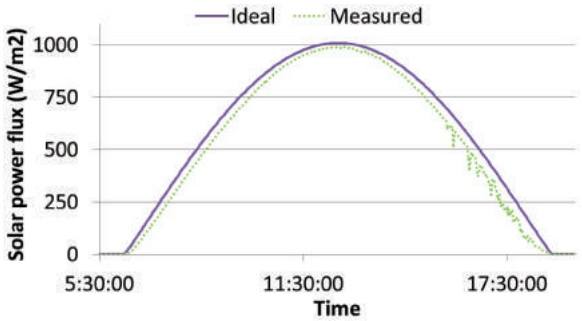

Fig. 2. Ideal and actual solar flux in Phoenix, Arizona on April 4, 2012 [NREL 2011].

solar power flux (also called the ideal solar flux) can be modeled from the physical properties (speed, rotation, shape, and so on) of the Sun and the Earth. The solar profile is then scaled by the panel size and the power conversion efficiency. We use the models from Michalsky [1988] and NREL [2000] to characterize the ideal solar radiation with the assumption that the solar panel converts the power with a 10% efficiency. The ideal and the actual solar fluxes for April 4, 2012 in Phoenix, Arizona [NREL 2011] are shown in Figure 2. We denote the power received from the solar panel at time t as $P_{sol}(t)$ which has already factored the panel's attributes (i.e., size, orientation, efficiency, etc.). Note the accuracy of the solar profile directly impacts the performance of the solution provided in this article. If the predicted solar profile was to dramatically differ at some point during the operation period, the proposed solution would have to be rerun with the updated input. Additionally, computational power and network size limit the feasibility of rerunning the solution to meet real-time conditions. For the rest of this work, it is assumed that the solar profile is ideal; however, the solution method is applicable to any solar profile.

3.2. Sensor Characteristics

We consider a sensor system that consists of active sensors, such as ultrasonic sensors and radars. Such sensors operate by transmitting signals in the form of waves to detect the presence of a target. The sensor will receive either a response from the target

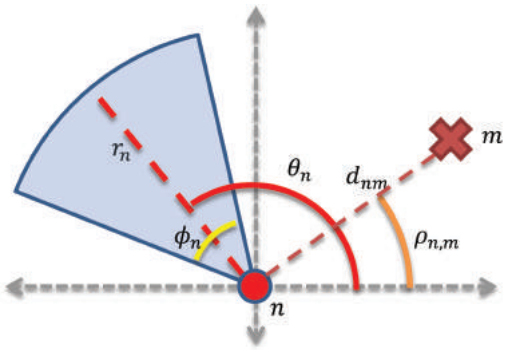

Fig. 3. An active narrow-beam sensor.

(if present) or the remnants of the reflected/scattered data that the sensor originally sent [Skolnik 1962]. The relationship between the sensor's transmission power (p_t) and its received power (p_r) can be expressed as [Friis 1946]

$$\frac{p_r}{p_t} = G_r G_t \left(\frac{\lambda}{4\pi r_n}\right)^{\alpha}, \tag{1}$$

where G_t and G_r are the transmit and the receive antenna gains, λ is the signal wavelength, α is a path-loss exponent (between 2 and 6), and r_n is the distance between the transmitter and the receiver. For simplicity, interference between simultaneously active sensors is ignored. Such interference can be managed by the underlying MAC layer (e.g., through an appropriate TDMA or FDMA mechanism).

For given antenna gains, receive-power threshold, and scattering conditions, the power consumption of sensor n sensing distance r_n can generally be expressed as

$$p_{sen,n}(r_n) = \beta_n r_n^{\alpha_n} + \mu, \tag{2}$$

where the values of α_n and β_n reflect the properties of the sensor, and μ is the average power requirement of all other system components. A vector form of this function is represented by $\mathbf{p}_{sen}(\mathbf{r})$ for all sensor nodes in the network. Similarly, this style of notation extends to other variables used in this work.

In many active sensor networks, there is no constant act of sensing, but rather a periodic process in which the sensor transmits to determine a target's state and then enters into a low-power state to conserve energy. As such, it is beneficial to model the sensor's energy consumption in the discrete domain. That is, if we assume that each sensing period is of length τ, also called *sampling interval*, then the energy drawn by sensor n during the kth interval $[k\tau, (k+1)\tau]$ is given by

$$e_{sen,n}(r_n(k)) = \delta\tau p_{sen,n}(r_n(k)) + (1-\delta)\tau p_{sen,n}(0), \tag{3}$$

where δ is the *beacon interval*, which represents the fraction of time spent actively sensing in an interval k. The beacon interval is assumed constant for a given sensor and a network setup. In (3), $r_n(k)$ is the value of r_n during the sampling interval $[k\tau, (k+1)\tau]$.

Sensors can operate in an omnidirectional or a narrow-beam coverage mode as illustrated in Figure 3. The area that a narrow-beam sensor n covers can be described as a sector which is specified by θ_n, the angle to the line in the middle of the sector, and a beamwidth ϕ_n. The directional heading of a target m with respect to sensor n is denoted by $\rho_{n,m}$. Note that as ϕ_n approaches 2π, the narrow-beam sensor becomes an omnidirectional sensor. In this work, ϕ_n and θ_n are assumed fixed and known for each sensor n.

3.3. Radio-Frequency Communication

In addition to sensing-related energy consumption, we also need to account for the energy used to communicate sensed data to the sink, possibly over a multihop WSN. In reality, such energy consumption depends on link budget, phase noise, startup time, data rate, channel fading, channel interference, etc. [Wang et al. 2001]. To simplify our model we assume that the energy consumption due to these effects is a constant average, which is a function of the number of packets sent. With this simplification, the routing path remains the only key factor in determining communication energy requirements.

Given the model in (1) and the locations of all N sensor nodes, the minimum transmission power required to send a message from one node to another can be calculated. Given these transmission power requirements as well as the time required to transmit one bit of data, it is straightforward to calculate $e_{tx,(i,j)}$, the energy per message needed to transmit data from sensor i to sensor j. The corresponding $N \times N$ matrix for all i and j is denoted E_{tx} where the values along the diagonal are zeros. Additionally, the energy required to receive a message e_{rx} is assumed constant for all sensors.

The final component of the network communication cost is the actual amount of data that is transmitted between two sensor nodes, which can be conveyed as an $N \times N$ "traffic matrix" $\boldsymbol{\chi}$. Here, the element $\chi_{i,j}$ of $\boldsymbol{\chi}$ represents the number of messages sent from sensor i to sensor j. The total energy expended on RF communications by sensor n in the kth time interval $[k\tau, (k+1)\tau]$ is given by

$$e_{com,n}(k) = \sum_{i=1}^{N} e_{tx,(n,i)}\chi_{n,i}(k) + \sum_{i=1}^{N} e_{rx}\chi_{i,n}(k), \tag{4}$$

where $\chi_{n,n}(k) \stackrel{\text{def}}{=} 0$. One should note that many sensor networks may also have timing constraints on data delivery. In this work, such constraints are ignored to arrive at a simpler solution methodology, but the proposed solution can accommodate such requirements. Although our communication model does not explicitly capture the energy expenditure due to packet losses and retransmissions, this can be easily be factored into E_{tx} and e_{rx}.

Other assumptions that we make related to RF communications made in this work are as follows.

—Each sensor node uses a *fixed* transmission power to communicate its sensed data to another sensor node, that is, dynamic power control is not implemented for sensor-to-sensor communications.
—A fixed PHY-layer transmission rate R (in bits/second) is used for the communications part.
—The network is not heavily loaded, so that a node i can complete its transmission to another node j within the sampling interval τ (more formally, the transmission time $L\chi_{i,j}(k)/R$ is less than τ, $\forall i, j, k$, where L is the length of a message in bits). This assumption is consistent with the low duty-cycle of typical WSNs.
—The message size is fixed.

3.4. Battery Model

For simplicity, we adopt a linear battery model (linear charging and discharging) with no energy loss or leakage in this work. However, a more realistic model including one that accounts for *rate-dependent capacity* and temperature dependence [Rakhmatov et al. 2003; Rao et al. 2003; Rakhmatov and Vrudhula 2003] can be accommodated. For short-term operations, such as the 24-hour target monitoring application addressed in

this article, the benefits of using a more complicated battery model may not warrant the increased complexity associated with it.

For a given sensor n, the energy that can be provided by the battery at the beginning of interval k is obtained by adding the current solar energy to the remaining battery energy and subtracting the communication and the sensing energy as shown next.

$$e_{bat,n}(k) = e_{bat,n}(k-1) + \int_{(k-1)\tau}^{k\tau} p_{sol}(t)\, dt - [e_{sen,n}(r_n(k)) + e_{com,n}(k)], \tag{5}$$

Note that the sampling time intervals for the radio communication and sensing phases are the same. Additionally, the battery is constrained to $[e_{bat}^{-}, e_{bat}^{+}]$, which denote the minimum required battery energy and the maximum charging capacity of the battery, respectively.

3.5. Cover Model

A cover model defines the total number of targets covered as a function of the sensing radius. A sensor is said to cover a target if the target lies within the sensing region of that sensor. We define the cover function of a target m and narrow-beam sensor n as

$$\zeta(r_n, n, m) = \begin{cases} 0, & \text{if } r_n < 2d_{n,m} \text{ or } \ \rho_{n,m} \notin [\theta_n \pm \phi_n/2], \\ 1, & \text{if } r_n \geq 2d_{n,m} \text{ and } \ \rho_{n,m} \in [\theta_n \pm \phi_n/2], \end{cases} \tag{6}$$

where $d_{n,m}$ is the distance between sensor n and target m. The expression $r_n \geq 2d_{nm}$ and $\rho_{n,m} \in [\theta_n \pm \phi_n/2]$ signifies the wedge corresponding to the sensing region of sensor n given its radius r_n and whether this region encapsulates the location of target m. The necessity of the constant factor 2 stems from the fact that the sensing signal from an active sensor must travel to the target and be reflected back to the sensing unit. For simplicity, we assume that the effects of scattering due to the reflection process can be incorporated into α_n and β_n terms of the sensor power equation (2). An example of these values is shown in Figure 3, where angles are measured with respect to the positive x-axis.

The total number of targets that are covered by one or more sensors in S (set of all sensor nodes) with radii $\mathbf{r}$ is given by

$$\zeta(\mathbf{r}) = \sum_{m \in T} \max_{n \in S}(\zeta(r_n, n, m)), \tag{7}$$

where T is the set of targets. For a given target m, $\max_{n \in S}(\zeta(r_n, n, m))$ is either 0 if no sensor covers m, or 1 if at least one sensor covers m. Hence, the sum over m is the total number of covered targets for the given radius profile $\mathbf{r}$.

Figure 4(a) shows an instance of a 1D sensor network (sensors and targets are placed along a line), and Figure 4(b) shows the corresponding cover function ζ. Notice the discrete nature of the cover function with respect to the sensing radius.

It should be noted that while this article assumes radial and wedge-shaped sensing regions, our solution can accommodate other models of ζ, including the cases where occlusions are present. The only requirement is that the effects of these occlusions are known and the resulting ζ is nondecreasing with respect to the sensing radii.

Furthermore, the definition of ζ may be extended to accommodate mobile targets. In this case, one may use, for example, the predicted target locations to derive the solution. However, much like the case of uncertain solar profiles, if the target location significantly varies over time, then the algorithm must be rerun to reflect this new information. Thus, if the predicted target locations change too rapidly, our solution is not computationally feasible. Another important version of coverage is known as *area coverage* or *field coverage*. For this case, two approaches may be considered. First, the

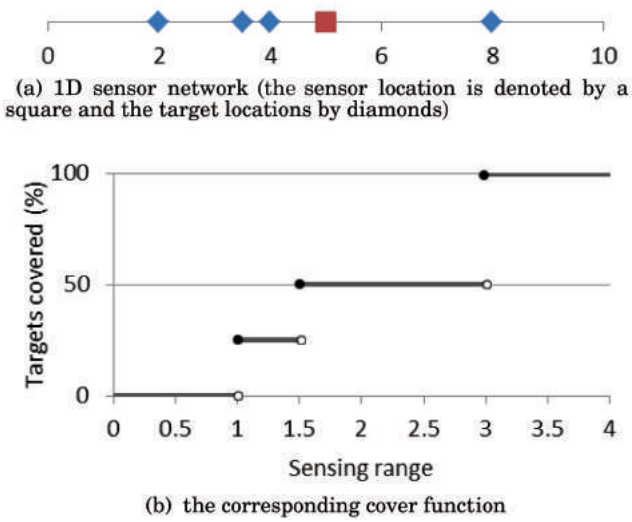

(a) 1D sensor network (the sensor location is denoted by a square and the target locations by diamonds)

(b) the corresponding cover function

Fig. 4. 1D sensor network and its cover function.

region to be covered can be approximated by a large number of target points. Second, one may modify the definition of ζ to denote the percentage of covered area [Huang and Tseng 2003].

4. THE MAXIMUM QUALITY OF COVER PROBLEM

In this section, we present the mathematical formulation for the maximum QoC problem. A summary of our notation is given in Table I. Vector quantities are shown in **bold** font, while matrices and sets are shown in uppercase. Subscripts are used whenever there is a need to index elements over a set.

4.1. Problem Description

The QoC of a network, denoted by ζ_{min}, is defined as the minimum value of $\zeta(\mathbf{r}(k))$ over a 24-hour duration, namely, $\zeta_{min} = \min_{k\in\{0\ldots K\}} \zeta(\mathbf{r}(k))$. QoC is additionally constrained by the condition that all sensors monitoring a target must have a route to the sink in order to report their data. This means that there must be a path from a sensor to the sink such that all sensors along this path have enough energy to sustain the required transmissions. In the example in Figure 5, a cover is found with a radius profile $r_1 = 2$, $r_2 = 2$, $r_3 = 0$, and $r_4 = 1$. If every point in the grid is a target, then $\zeta_{min} = 16$. This would be a valid cover if S_1, S_2, S_4 have a routing path to the sink. The problem specification demands such covers be computed for the entire operational time, while maximizing ζ_{min}. The concept of maximizing ζ_{min} is of vital importance in many critical sensor network applications. Periods of low coverage represent periods of vulnerability in the network. If the objective was to maximize the average ζ over an operational period, there may be periods of low ζ and periods of high ζ. For example, in the application of military battlefield surveillance the periods of low ζ would represent a time when a large portion of the battlefield is unobservable and thus vulnerable to attack.

The maximum QoC problem is defined as follows: Given a set of sensor nodes and a set of targets, find a subset of sensor nodes, their corresponding sensing radii, and a corresponding routing strategy that maximize the QoC for the entire operational time

Table I. Notation

S	Set of sensor nodes and their locations
N	Number of sensor nodes
$\mathbf{T}$	Set of targets and their locations
M	Number of targets.
$r_n(k)$	Radius used by sensor n during the time interval k
$e_{bat,n}(k)$	Battery charge of sensor n at the start of time interval k
$p_{sen,n}(r)$	Power usage of sensor n at radius r
$e_{sen,n}(r)$	Energy usage of sensor n at radius r for one time interval
δ	Fraction of time spent sensing during a time interval
τ	Length of a discrete time interval
$p_{sol}(t)$	Power delivered by a solar panel at time t
$e_{tx,(i,j)}$	Joules per message needed to transmit data from sensor i to sensor j
e_{rx}	Joules per message needed for a sensor to receive data
$e_{com,n}(k)$	Radio energy usage of sensor n during time interval k
$\chi_{i,j}(k)$	Number of messages sent from sensor i to Sensor j during time interval k
$D_n(k)$	Total number of messages generated by sensor node n during time interval k
$\mathbf{D}(k)$	Total number of messages in the network during time interval k
$S_{on}(k)$	The set of sensors monitoring some target during time interval k
$S_{off}(k)$	The set of sensors not monitoring any target during time interval k
S_0	The centralized base station (communication sink)
$\zeta(\mathbf{r})$	Number of targets covered with sensor radii $\mathbf{r}(t)$
$d_{n,m}$	Distance between Sensor n and Target m
θ_n	Beam angle (direction) of sensor n
ϕ_n	Beamwidth of sensor n
$\rho_{n,m}$	Angle between target m and Sensor n
K	Total number of time intervals in 24 hour period

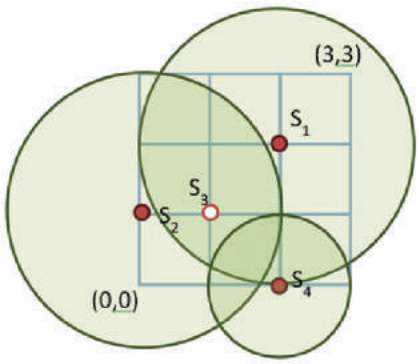

Fig. 5. Valid cover. Each grid point is a target.

of the network. Mathematically, the problem can be stated as follows.

$$\underset{\{\mathbf{r}(k),\boldsymbol{\chi}(k)\}}{\text{maximize}} \quad \zeta_{min} = \min_{k\in\{0\ldots K\}} \zeta(\mathbf{r}(k)) \tag{8}$$

$$\text{such that} \quad \mathbf{e}^{-}_{bat}(k) \le \mathbf{e}_{bat}(k) \le \mathbf{e}^{+}_{bat}(k), \ \forall k \tag{9}$$

$$e_{bat,n}(k) = e_{bat,n}(k-1) + \int_{(k-1)\tau}^{k\tau} p_{sol}(t)\,dt - [e_{sen,n}(r_n(k)) + e_{com,n}(k)] \tag{10}$$

$$e_{sen,n}(r_n(k)) = \delta\tau p_{sen,n}(r_n(k)) + (1-\delta)\tau p_{sen,n}(0),\ \forall n \in S \tag{11}$$

$$\sum_{j=1}^{N} \chi_{j,i}(k) - \sum_{j=1}^{N} \chi_{i,j}(k) = 0,\ \forall i \in S_{off}(k),\ \forall k \tag{12}$$

$$\sum_{j=1}^{N} \chi_{j,i}(k) - \sum_{j=1}^{N} \chi_{i,j}(k) = -D_i(k),\ \forall i \in S_{on}(k),\ \forall k \tag{13}$$

$$\sum_{j=1}^{N} \chi_{j,i}(k) - \sum_{j=1}^{N} \chi_{i,j}(k) = \sum_{j \in S_{on}(k)} D_j(k),\ \forall i = S_0,\ \forall k \tag{14}$$

$$e_{com,n}(k) = \sum_{i=1}^{N} e_{tx,(n,i)}\chi_{n,i}(k) + \sum_{i=1}^{N} e_{rx}\chi_{i,n}(k),\ \forall k \tag{15}$$

In the preceding formulation, the constraint equation (9) prevents the battery energy of any sensor from falling below a specific threshold, while (10) describes the charge/discharge behavior of the battery. Constraints (12)–(14) are standard flow conservation constraints that ensure that all messages $\mathbf{D}(k)$ created by active sensors $S_{on}(k)$ during time interval k are delivered to the sink S_0. Each active sensor in the set $S_{on}(k)$ is assumed to be periodically sensing and transmitting data; as such, the value of $D_i(k)$ is directly related to the frequency of this transmission. These constraints are well established and represent any network flow [Papadimitriou and Steiglitz 1982]. Sensors that are not actively sensing during the interval k are part of $S_{off}(k)$, and may be used as relay nodes between the nodes of $S_{on}(k)$ and S_0. The optimization parameter is the vector of time-varying sensor radii $\mathbf{r}(k)$ and the traffic matrix $\boldsymbol{\chi}(k)$. The previous formulation falls under the realm of nonlinear optimal control problems [Kirk 1970].

Nonlinear optimal control problems of the aforesaid type are computationally hard to solve, and the runtimes do not scale well with the size of the network. Conventional solution techniques are based on dynamic programming (DP) and the Hamilton-Jacobi-Bellman method [Kirk 1970]. To solve this problem using DP, the entire duration of execution (the 24-hour period) must be partitioned into K time intervals. Furthermore, discretization of the states and the controls is also needed. Let Q_b denote the number of discrete states for the battery level and let Q_r be the number of discrete sensor radii. Furthermore, there are at most N^2 possible communication links between sensors (in a fully connected topology). With the preceding, the runtime complexity of the DP solution would be $O(K(Q_b)^N(Q_r + N^2)^N)$ for an N-sensor network, since the solution requires examining all possible controls at every possible state.

The problem at hand has some special characteristics that enable us to solve it near optimally and in a less intensive computational way compared with the DP solution.

4.2. Solution Outline

The problem formulation described in Eqs. (8)–(15) have several important characteristics that will be utilized to derive the solution method.

(1) For a given interval k, the objective function (8) is a discrete monotonic function in $\mathbf{r}$, as observed in Figure 4(b). Any monotonic function is also a quasilinear function, that is, it is both quasiconvex and quasiconcave.
(2) For any given $\mathbf{r}(k)$, there are potentially many possible $\boldsymbol{\chi}(k)$ that may satisfy constraints (12)–(15); however, each $\boldsymbol{\chi}(k)$ will directly impact the residual battery levels at the start of the time interval $k+1$ and thus impact the QoC of the network.

Therefore, it is reasonable to assume that the best value of $\boldsymbol{\chi}(k)$ is one that satisfies (12)–(15) while maintaining the highest residual energy in the sensor batteries.

(3) The solution space R consists of a set of vectors $\mathbf{r}(k)$. Let $R^* \subseteq R$ denote the set of optimal solutions. R^* consists of feasible (satisfy the constraints) functions $\mathbf{r}^*(k)$ whose corresponding minimum coverage $\zeta(\mathbf{r}^*(k))$ is larger than the minimum coverage of any other feasible function $\mathbf{r}(k)$. Therefore, among the solutions in R^*, we prefer the one that deviates the least from ζ_{min} at every time interval k, as there is no added benefit of having a larger cover than ζ_{min} (since this does not improve the value of the objective function).

It is the last observation that is key to the transformation of the formulation. Since every $\mathbf{r}^*(k) \in R^*$ is such that $\zeta(\mathbf{r}^*(k)) \geq \zeta_{min}$ (an unknown constant within a known range) and there is no benefit in exceeding this value at any point in time, the optimization problem (8)–(15) can then be solved using a binary search over the values of ζ_{min}, and for each such choice of ζ_{min}, a quasiconvex optimization problem to determine $\mathbf{r}(k)$ and $\boldsymbol{\chi}(k)$ to achieve the specified ζ_{min} coverage is solved. If no feasible solution is found, ζ_{min} is lowered; otherwise, it is increased to determine the next maximum ζ_{min}. Since the objective is now transformed into a constraint, a new objective function needs to be defined, for example, maximizing the total residual battery energy in the network or maximizing the minimum sensor node battery energy.

Figure 6 outlines of the proposed optimization algorithm. The steps of the algorithm are explained next.

Step 1: A binary search over all possible ζ_{min} is performed. ζ_{min} is initialized to half the total number of targets ($||T||$).

Steps 2–3: The interval of operation (e.g., 24 hours) is discretized into time intervals $1, 2, \ldots, K$. For each time interval k, within each iteration of the binary search, the tentative optimal value of $\mathbf{r}(k)$ is computed via a gradient search of the objective, while satisfying the constraints. An initial value of $\mathbf{r}$ is assumed to begin the search of $\mathbf{r}(0)$.

Step 4: Given $\mathbf{r}(k)$ (which may not be optimal), a feasible $\boldsymbol{\chi}(k)$ is determined for (27)–(34). With the assumed $\mathbf{r}(k)$ and the corresponding $\boldsymbol{\chi}(k)$, an associated objective cost (19) is calculated along with its feasibility constraints through Eqs. (20)–(26). Finally, the corresponding gradients for Eqs. (19)–(26) are calculated.

Step 5: $\mathbf{r}(k)$ is updated based on the gradients computed in the previous step [Nocedal and Wright 2000].

Step 6: Due to the numerical nature of the gradient search, the stopping criterion for finding the minimum objective in (19) is based on user-provided tolerances. Steps 4 and 5 are executed until a solution within the given tolerances is found or until it is determined that no feasible solution exists.

Steps 7–8: If no feasible solution is found during the gradient search procedure in steps 4–6, then it is not possible to achieve a QoC greater than ζ_{min}. Consequently, ζ_{min} is reduced through a binary search.

Step 7–11: If a feasible solution is found during the gradient optimization procedure in steps 4–6, then a ζ_{min} coverage is achievable up to time period k. Steps 4–10 are repeated until ζ_{min} is determined to be valid for all time instants up to K. An affirmative result means that a solution with a minimum cover ζ_{min} is possible, and ζ_{min} can be increased according to the binary search algorithm.

Note if the constraints (9)–(15) are infeasible, then no solution exists. In this event, we set all sensors into a sleep mode, where the sensors' sensing ranges are set to 0 and

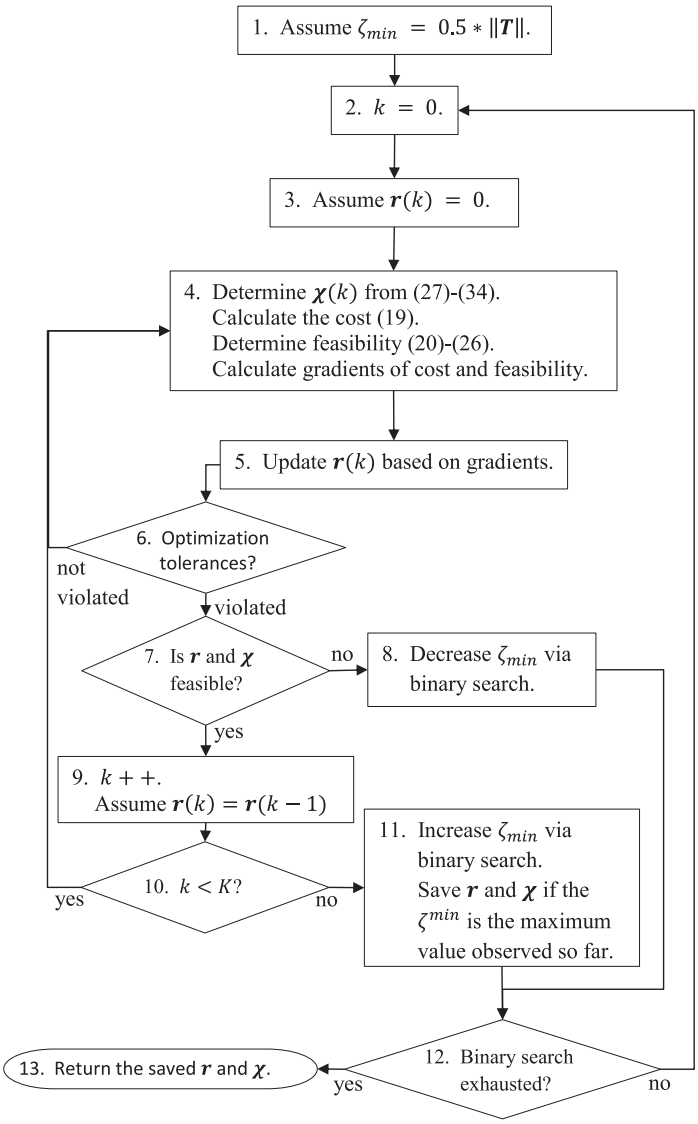

Fig. 6. Outline of the proposed solution to maximize QoC.

have no communication. This is to allow the batteries to recharge via the solar panel and possible achieve some level of QoC at a future point outside of the operating range $k \in [0 \ldots K]$.

5. IMPLEMENTATION DETAILS

In this section, the details of the quasiconvex optimization formulation for the k^{th} interval, $1 \leq k \leq K$ (steps 3–6 of Figure 6) are presented.

5.1. Quasiconvex Optimization Solution for Determining r

The discrete function $\zeta(\mathbf{r}(k))$ in (7) is first replaced by a continuous approximation. This is necessary for gradient-based solution techniques to work, as they expect the

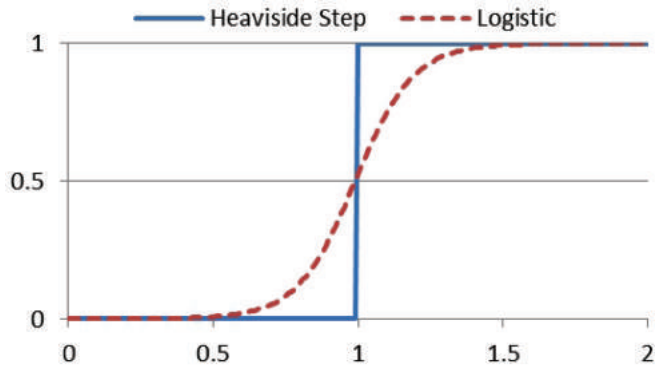

Fig. 7. The Heaviside Step function and the Logistics function.

objective and all constraints to be smooth and differentiable. Towards this, the discrete jumps (which are defined by the *Heaviside Step* function) in the cover function (see Figure 4(b)) are approximated by the *Logistics* function, as shown in Figure 7. The resulting cover function is

$$\zeta(\mathbf{r}(k)) = \sum_{m \in T} \max_{n \in N} \left(L(r_n/2d_{n,m})\right), \tag{16}$$

$$L(x) = \frac{1}{1 + e^{-c \cdot x + \delta}}, \ \forall x \in (0, 1), \tag{17}$$

$$\delta = \ln(1/\epsilon - 1) + c. \tag{18}$$

$L(x)$ is the Logistics function. Since x in (17) is bounded, r_n in (16) gets normalized by $d_{n,m}$. The constants c and ϵ are quality factors, used to control how closely the Logistics function resembles a step function. Increasing these values provides a better approximation, but at the cost of increased solution time for the optimizer. Now the function $\zeta(\mathbf{r}(k))$ is continuous both in its domain and in its range, thus allowing a gradient search method to compute the necessary derivatives and traverse over the feasible search space of the problem.

Since the optimal objective function in (8) is now treated as a constraint, the original objective needs to be substituted with an objective that also improves the QoC. Of the several possibilities, minimizing the total sensing energy is a good candidate. With this, the quasiconvex formulation for determining $\mathbf{r}$ for a k^{th} interval is given by

$$\underset{\mathbf{r}(k)}{\text{minimize}} \quad \sum_{n=1}^{N} P_{sen,n}(r_n(k)) \tag{19}$$

$$\text{such that} \quad e_{bat,n}(k) = e_{bat,n}(k-1) + \int_{(k-1)\tau}^{k\tau} p_{sol}(t)\, dt - e_{sen,n}(r_n(k)) - e_{com,n}(k) \tag{20}$$

$$\mathbf{e}^{-}_{bat}(k) \leq \mathbf{e}_{bat}(k) \leq \mathbf{e}^{+}_{bat}(k) \tag{21}$$

$$\zeta(\mathbf{r}(k)) = \sum_{1}^{M} \max_{n \in N} \left(L(r_n/2d_{n,m})\right) \tag{22}$$

$$\zeta(\mathbf{r}(k)) \geq \zeta_{min} \tag{23}$$

$$L(x) = \frac{1}{1 + e^{-c \cdot x + \delta}}, \quad \delta = \ln(1/\epsilon - 1) + c \tag{24}$$

$$e_{sen,n}(r_n(k)) = \delta \tau p_{sen,n}(r_n(k)) + (1 - \delta)\tau p_{sen,n}(0), \ \forall n \in S \tag{25}$$

$$e_{com,n}(k) = \sum_{i=1}^{N} e_{tx,(n,i)} \chi^*_{n,i}(k) + \sum_{i=1}^{N} e_{rx} \chi^*_{i,n}(k), \ \forall n \in S. \tag{26}$$

The objective function (19) is to minimize the total power spent by the network during each interval k of length τ. Constraint (23) requires that the minimum cover be above a specific level. The other constraints are the same as in Eqs. (9)–(11). It is easy to show that the preceding equations are convex, except for Eqs. (22) and (24). Logistic functions are monotonic functions. Hence, they are also quasiconvex functions [Boyd and Vandenberghe 2004]. Since `sum` and `max` are convex functions when their inputs are monotonic, Eq. (22) is a quasiconvex function. This makes the previous formulation a quasiconvex optimization problem.

In the aforesaid formulation, it is assumed that the optimal routing table $\boldsymbol{\chi}^*(k)$ is computable for a given $\mathbf{r}(k)$. $\boldsymbol{\chi}(k)$ needs to be solved for each assumed $\mathbf{r}(k)$ during the gradient search process. Alternatively, one may directly include $\boldsymbol{\chi}(k)$ along with constraints (12)–(14) in the convex optimization process. However, convex optimizers tend to be inefficient as the number of control variables increases. In this case, the number of elements of $\boldsymbol{\chi}(k)$ is upper-bounded by N^2. To reduce the computation time, $\boldsymbol{\chi}(k)$ is determined independently from $\mathbf{r}(k)$ by solving a linear programming problem.

5.2. Linear Programming Solution to Determine χ

This section describes a method to determine the feasibility of connectivity for a given $\mathbf{r}(k)$ and to determine the optimal traffic matrix (with respect to objective (19)), if one exists.

In order to successfully route sensed data through the network to the sink, one must first define which sensor nodes are sources. A sensor node is defined to be a source of data for the k^{th} interval if it is uses a sensing radius greater than 0. Such a node belongs to the set $S_{on}(k)$. For this reason, the radius profile must be known before a valid routing scheme can be found. Thus, connectivity may be viewed as a subproblem of the target cover problem.

A valid connectivity is found as the solution to the following Linear Program (LP)

$$\underset{\boldsymbol{\chi}(k)}{\text{minimize}} \quad \sum_{n=1}^{N} e_{com,n}(k) \tag{27}$$

$$\text{such that} \quad \chi_{i,j}(k) \geq 0, \ \forall i, j \in S, \tag{28}$$

$$\sum_{j=1}^{N} \chi_{j,i}(k) - \sum_{j=1}^{N} \chi_{i,j}(k) = 0, \ \forall i \in S_{off}(k), \tag{29}$$

$$\sum_{j=1}^{N} \chi_{j,i}(k) - \sum_{j=1}^{N} \chi_{i,j}(k) = -D_i(k), \ \forall i \in S_{on}(k), \tag{30}$$

$$\sum_{j=1}^{N} \chi_{j,i}(k) - \sum_{j=1}^{N} \chi_{i,j}(k) = \sum_{j \in S_{on}(k)} D_j(k), \ \forall i = S_0, \ \forall k, \tag{31}$$

Table II. Default Parameter Values

Param	Value	Param	Value	Param	Value	Param	Value
r_{max}	10 m	radio: α	3.14	sensor: α	4.00	Panel Size	5 cm^2
$B(0)$	0.72 kJ	radio: β	0.0002	sensor: β	0.0000138	Area	15 m^2
e^+_{bat}	4.32 kJ	radio: μ	0.003	sensor: μ	0.007	e^-_{bat}	0 kJ
K	48	radio freq.	2.4 GHz	message size	64 bits	τ	30 min.
δ	1	ϕ	2π				

$$e_{com,n}(k) = \sum_{i=1}^{N} e_{tx,(n,i)}\chi_{n,i}(k) + \sum_{i=1}^{N} e_{rx}\chi_{i,n}(k), \tag{32}$$

$$e_{bat,n}(k) = e_{bat,n}(k-1) + \int_{(k-1)\tau}^{k\tau} p_{sol}(t)\,dt - e_{sen,n}(r_n(k)) - e_{com,n}(k), \tag{33}$$

$$\mathbf{e}^-_{bat}(k) \le \mathbf{e}_{bat}(k) \le \mathbf{e}^+_{bat}(k), \tag{34}$$

where $D_i(k)$ is the amount of data (messages) generated by a source node i which must be sent to the sink; $\boldsymbol{\chi}(k)$ is an $N \times N$ matrix corresponding to the desired routing path (note that $\chi_{i,j}(k)$ is the amount of data sent from node i to node j). Constraints (29)–(31) simply ensure that all the transmitted data is delivered to the sink.

When solving for the traffic matrix as an LP, error is introduced due to the discrete nature of the composition of packets. Furthermore, as discussed in Section 3.3, $\boldsymbol{\chi}(k)$ may have to be integer valued if the overhead of message splitting/merging is not negligible. Should these factors play a significant role in the energy consumption of the sensor node, integer programing (IP) methods such as cutting-plane and sequential fixing [Papadimitriou and Steiglitz 1982] will be required. These lack the computational efficiency of LP solvers, but will provide much more accurate solutions.

6. SIMULATION RESULTS

6.1. Simulation Setup

The proposed solution for the maximum QoC problem was verified by simulating a stationary network of sensor nodes and targets in various configurations. A flat, square sensing field is assumed. The default parameter values are given in Table II. Radio parameter values are based on the data provided in the datasheet of TI's ez430-RF2500 wireless sensor node [eZ4 2009] and all sensor parameter values are based on Cassegrain Antenna series [ELVA-1 2012] datasheet.

The parameter $D_i(k)$ denotes how much traffic an active sensor i generates; however, for our simulations we assume that an active sensor generates one message per monitored target, which needs to be delivered to the sink. As such, there can be duplicate messages when a target is sensed by more than one sensor.

For all experiments, the sink location is assumed at coordinate $(0, 0)$, namely, the bottom-left corner of the square area. Since the locations of the sensors and the targets are known in advance, the values of $e_{tx,(i,j)}$ can be determined a priori using the methodology in Section 3.3 along with the data provided in Table II. Additionally, it is assumed that once the sink makes a scheduling decision (by solving the optimization problem), it notifies each sensor using direct communication (i.e., no routing). This assumption is valid as the sink is not power constrained and as such the overhead for each sensor node is one message, which is very low. Unless mentioned otherwise, this configuration is used in all subsequent experiments.

For simplicity, our experiments assume a homogeneous sensor network. However, this is not a limitation of the proposed method. The solar profile used in the experiments is shown in Figure 2. For each interval k, active sensors generate one 64-bit packet per monitored target. To highlight the benefits of the proposed solution, network topologies

were configured in such a manner that a 100% coverage is not achievable in trivially small networks ($N < 100$).

6.2. Sample Scheduling of the Proposed Algorithm

Figure 8 shows the plots of sensor radii over time as determined by the proposed algorithm, the resulting battery charge, and the QoC over a course of 24 hours. The network is configured with 3 sensors and 25 targets, arranged in a random pattern, as shown in Figure 8(a). The initial battery level for each sensor is 11J. In the interest of clarity, only 3 hours of the radii schedule are shown. Note that the algorithm switches between various covers with different radii to ensure that no battery runs out of energy while attaining the maximum possible QoC. This can be observed at time 2:30 am when the battery energy of Node 2 depletes completely and Node 3 increases its sensing radius to satisfy the QoC (see Figure 8(b)). Figure 8(e) shows that the battery primarily charges during hours of sunlight and rapidly discharges at night, as expected. The QoC of this schedule is kept constant at 3 targets.

6.3. Analysis of Traffic Routing Matrix $\boldsymbol{\chi}$

To complement the results in Section 6.2, this section presents the results for another small and simple network with a focus on the analysis of the traffic routing matrix $\boldsymbol{\chi}$ and how this matrix is impacted by the sensing radii. For this simulation, we choose a network consisting of 36 targets spread out uniformly over a 15 m $\times$ 15 m area. Targets are monitored by 4 sensor nodes with locations as shown in Figure 9(a). Each sensor reports one message per interval for each monitored target. Sensing ranges are limited to 7.5 m. Due to the small network size (in terms of number of sensors, traffic volume, and physical area), network overhead is minimal ($\sim$1 μJ/message in the worst case). As such, we modified the radio parameter values to $\alpha = 6$ and $\beta = 0.5$ to create a scenario where sensing and RF energy costs are comparable. Additionally, e^{+}_{bat} was scaled to 75J for the same reasons.

Figures 9(b), 9(c), and 9(d) depict the battery-charge level, per-link communication traffic, and sensing radii, respectively, as a function of time. For this network, the algorithm determined a maximum QoC of 6 targets out of 36 using three different values of $\mathbf{r}$ and two different values of $\boldsymbol{\chi}$. From the operational start time until time 12:30 am, the algorithm determined that using sensor Node 1 to both sense targets and to route all other node's data was optimal with respect to the objectives (19) and (27). This cover remains valid until Node 1's battery energy is no longer sufficient to sustain both the sensing and routing duties. It is important to note that, even though Node 2 is not actively monitoring any target during this time, it is serving as a relay node to reduce the communication overhead for Nodes 3 and 4. Because the battery of Node 1 is exhausted to the point where no messages can be routed through it at time 12:30 am, Node 2 becomes active and starts monitoring four targets to maintain the QoC of 6, at the same time maintaining its traffic routing responsibilities for Nodes 3 and 4 (see Figure 9(e)). Finally, at time 2:30 am, Node 2 exhausts its battery charge necessary to monitor the four targets; however, it still has enough charge left to act as a relay node for Nodes 3 and 4 (both of which now require a larger sensing radii to maintain the QoC of 6). This is shown in Figure 9(f).

From the preceding simulation, we can see how the traffic routing matrix must dynamically adapt to changing values of $\mathbf{r}$ and the residual battery energy.

6.4. Runtime Analysis

To verify the practicality of the proposed solution, its runtime is compared with the DP solution. DP is one of the few known methods to solve optimal control problems; however, it requires all its continuous variables (controls, states, time, etc.) to be discretized

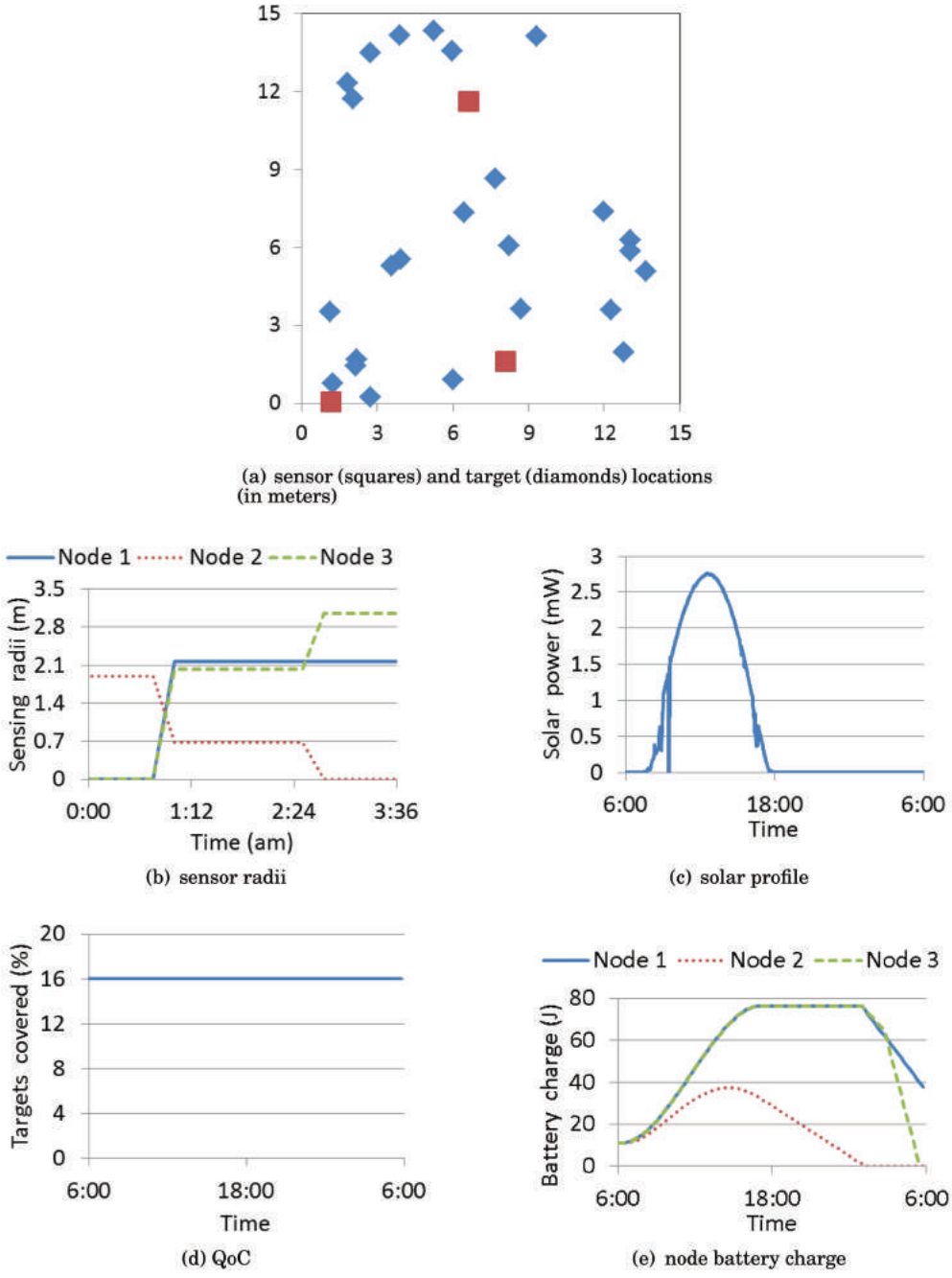

Fig. 8. Time plots of scheduling as determined by the proposed algorithm.

[Kirk 1970]. Increasing the number of quantized values for each of these variables will increase the accuracy of the result, but will require a longer execution time, as explained in Section 4.1. In contrast, the proposed solution assumes continuous control over sensing ranges. To ensure a fair comparison, the algorithm is modified to choose

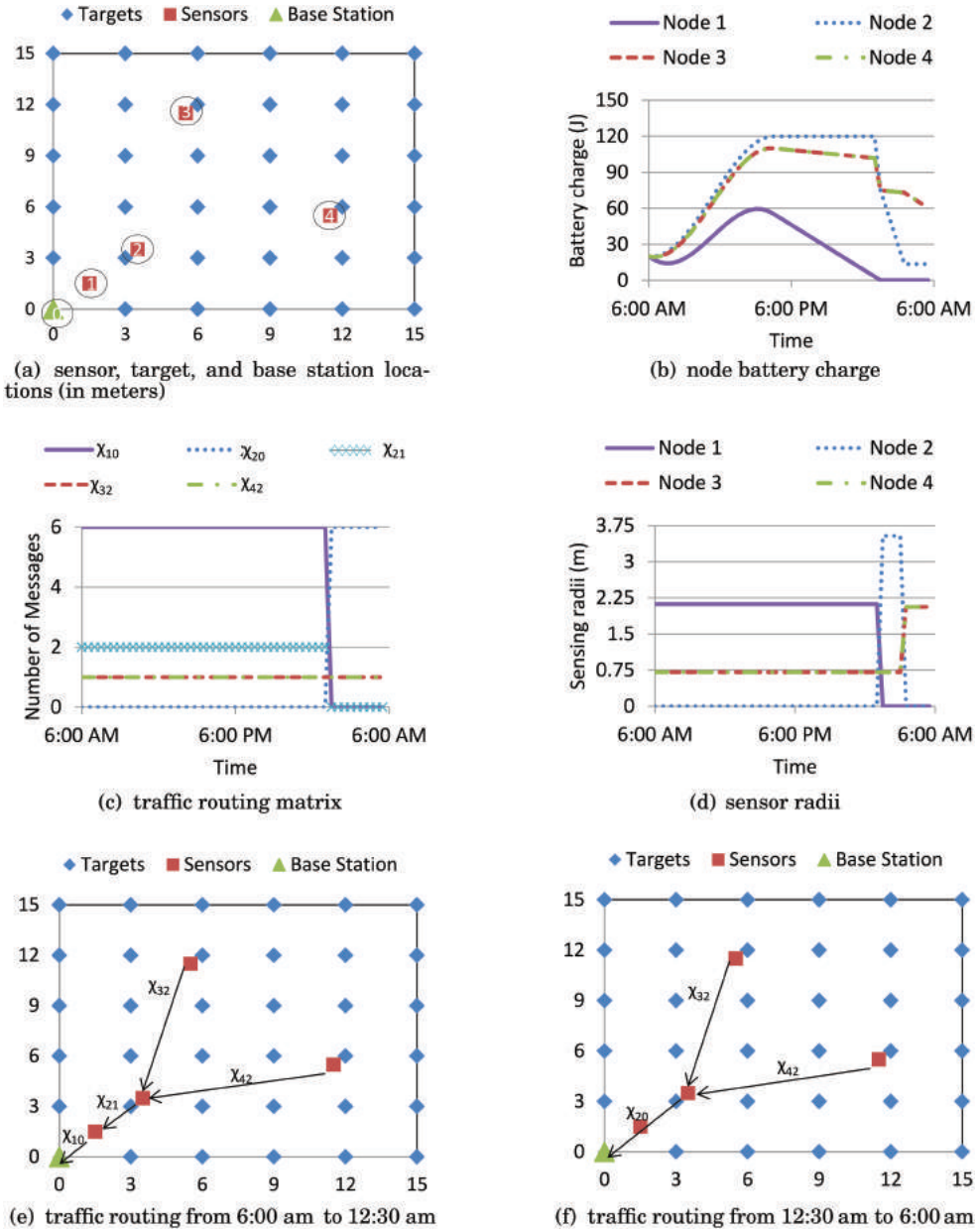

(a) sensor, target, and base station locations (in meters)

(b) node battery charge

(c) traffic routing matrix

(d) sensor radii

(e) traffic routing from 6:00 am to 12:30 am

(f) traffic routing from 12:30 am to 6:00 am

Fig. 9. Analysis of traffic routing for the proposed algorithm.

the nearest discrete range from a set of radii used in the DP solution. This is also required for a practical implementation of the proposed algorithm. All simulations are run on a single-core Dell workstation with 2.93 GHz Intel core i7 and a 8GB RAM.

In this experiment, sensors and targets are evenly distributed over an area of operation (see Figure 11(a)). The maximum number of sensor nodes is limited to five, due to the enormous computation time required by the DP solution. The battery charge is quantized with 7 states and the number of sensing ranges is kept constant at 6 for the

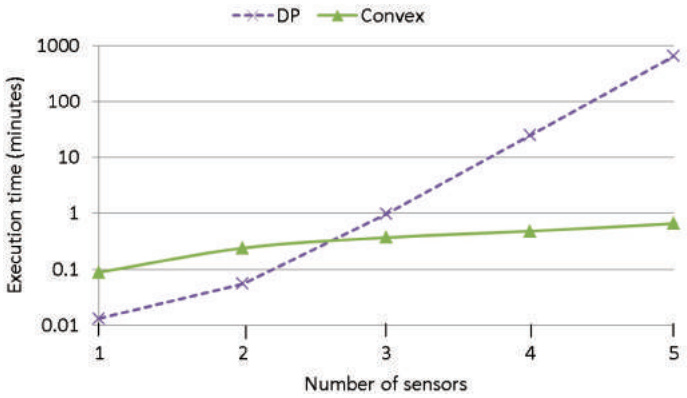

Fig. 10. Execution time vs. number of sensors.

Table III. Runtimes for Experiments Described in Section 6.4

N	1	10	20	40	50	100
Runtime	3.87 sec	100 sec	309 sec	21.2 min	33.2 min	2.12 hours

DP solution. Connectivity is not included in this experiment due to the exponentially increasing effect it has on the DP solution's state space.

The results of this experiment are shown in Figure 10. Notice that the y-axis has a logarithmic scale. We observe that as the number of senor nodes increases, the proposed solution achieves a significant speedup compared with the DP solution. Even for four sensor nodes, the quasiconvex optimizer finds a solution 60 times faster than the DP procedure. With such a speedup, one can use the proposed algorithm to explore the design space of the network in a reasonable time, as can be seen in the subsequent experiments. Table III demonstrates that the proposed solution can handle large networks and produce solutions in a reasonable time. Note that these runtimes are for a single-core processor. With the help of parallelization, it is possible to greatly reduce the runtimes.

The current proposed solution for maximizing the minimum coverage of a network requires an offline solution, and as such, is not adaptive to changing conditions. One suggestion on adopting the current solution to changing solar conditions is to rerun the algorithm with the updated solar input, with lower accuracy, thereby greatly decreasing computation time. The previous results suggest such a methodology is practical. If the predicted solar profile significantly changes at a rapid rate, one would have to explore alternative methods to solving this problem such as integrating Markovian chain predictors, which produces a result with a corresponding level of confidence.

6.5. Accuracy of the Proposed Solution vs. DP

The overall accuracy of the proposed solution against the naive DP solution outlined in Section 6.4 is examined here. Figure 11 shows three different sensor target location configurations. These configurations represent the diverse scenarios for a sensor network tasked with surveillance duty. Figure 11(a) illustrates the case where all targets and sensors are evenly distributed across the operational area for optimal area coverage. Figure 11(b) shows the case where all targets and sensors are evenly distributed across the area, but the sensors and the targets are separated from one another. This represents the scenario of an enemy territory surveillance. From an energy standpoint, this is one of the worst possible scenarios, as it requires larger sensing radii. Finally,

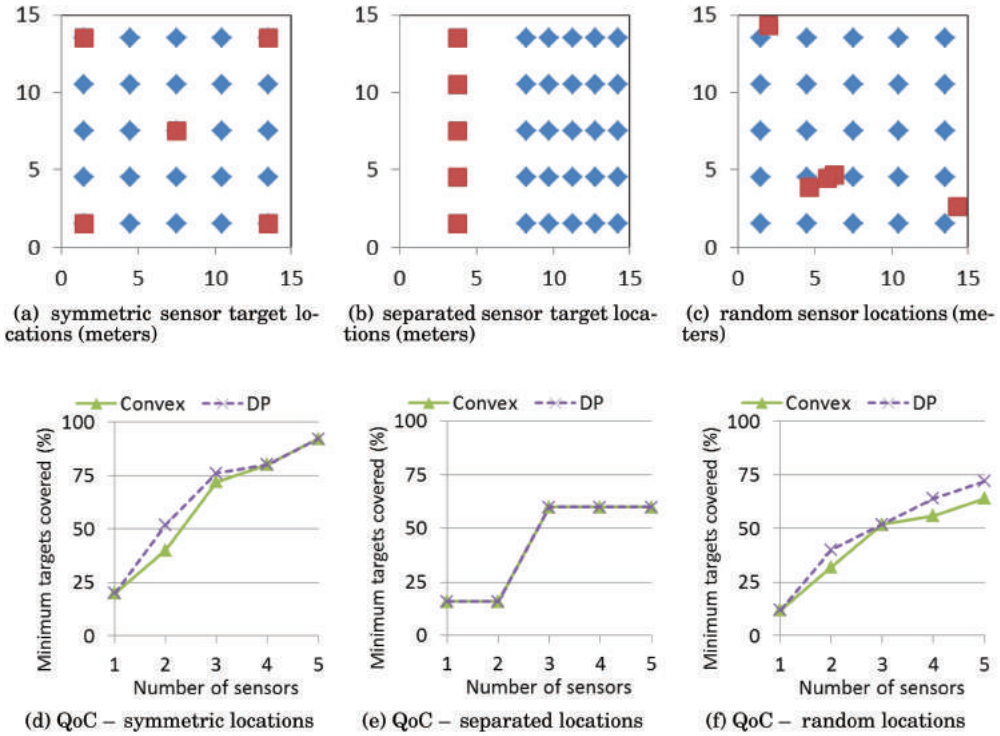

Fig. 11. Various layout scenarios and the resulting QoC.

Figure 11(c) shows the case where sensors are randomly distributed. This is the most common scenario in sensor networks tasked with monitoring inaccessible areas. For these experiments, the number of battery states is increased for the DP procedure to increase its accuracy. All other parameters remain the same as in Section 6.4.

The results in Figures 11(d), 11(e), and 11(f) show that the proposed algorithm can cope with several possible network scenarios and provide near-optimal results. For the symmetric configuration, as N increases, the proposed solution tends to provide almost identical results to the DP solution. This is due to the fact that as N increases, the mean distance from any sensor to any target decreases, thus allowing for smaller radii to be used. The results from both approaches converge due to reduction in the discretization errors for smaller radii. For the configuration in Figure 11(b), the two approaches give identical results. This may be attributed to the fact that there are far fewer valid covers for any given ζ_{min} in this configuration as opposed to the symmetric configuration. Finally, the random configuration tends to display varying levels of error at each value of N. This is to be expected, as sensor nodes randomly positioned create vastly different network topologies. Over the results of all experiments, a peak of 8% QoC loss is observed.

6.6. Impact of Connectivity on QoC and Execution Time

The goal of this experiment is to highlight the importance of considering connectivity and data routing alongside QoC. For this experiment a 21×21 grid of targets is placed over a 200 m $\times$ 200 m area. The number of sensors is varied and their locations are randomly chosen. To ensure equal contributions to the total cost, the values α and β for data transmission are altered such that the energy needed to sense a distance r for

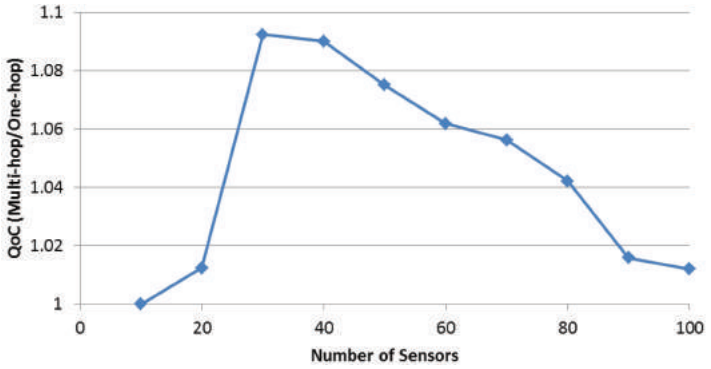

Fig. 12. Effect of connectivity on QoC.

one time interval is equivalent to the energy needed to transmit a message through a distance r.

Two routing schemes are considered. The first is a simple one hop routing scheme in which all active sensors simply transmit the data directly to the sink. Although naive, this method exhibits constant runtime. The second is the proposed algorithm presented in Section 5.2 which uses linear programming integrated into the quasiconvex optimization technique. This method is referred to as multihop routing. The results are shown in Figures 12 and 13.

As one would expect from an exponential power model, a one-hop routing scheme is inferior to multihop routing in terms of QoC. This is shown in Figure 12. Essentially, the communication energy is proportional to the distance traveled to the power of α, thus any additional overhead (due to additional sensors processing the message and to any additional distance the message must travel) is negligible. Thus the energy savings from the communication is able to be spent on covering additional targets which is ultimately the objective of the network. One should note, however, that as the sensor density increases, the degradation in QoC associated with the single-hop routing scheme diminishes. This is due to the fact that as the number of nodes increases, the total network energy also increases, therefore allowing more energy to be budgeted to communication. Furthermore, the impact on QoC is reduced when energy transmission costs become less significant in comparison to the sensor covering costs.

The time analysis is shown in Figure 13. Since the LP for connectivity must be solved for every guess of $\mathbf{r}$, the execution time increases substantially.

It can be concluded that introducing the connectivity constraints to the problem can improve QoC; however, it comes at the cost of increased execution time. As such, designers need to take careful note of the network size, power costs, and node density.

6.7. Effect of Sampling Interval τ and Beacon Interval δ on QoC

The sampling interval is the time between two consecutive sensing instants of an object and denoted as τ in Eq. (3). In many noncritical applications, targets do not require continuous monitoring, and for many sensor nodes continuous monitoring is impossible. For this reason, the sampling interval offers network designers a useful control variable to extend the lifetime of their networks at the expense of having periods of no coverage. In the context of solar-powered networks, the benefit is an increase in the QoC. In this experiment, the effect of increasing the sampling interval is investigated. Sensors and targets are arranged in a square grid-like pattern with equal spacing as shown in Figure 11(a). The number of sensors is kept constant at 100 and the number of targets is kept constant at 900, deployed over a 200 m $\times$ 200 m area. The sampling

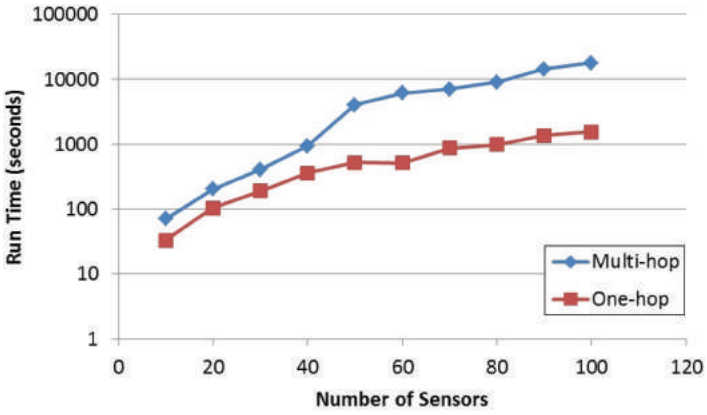

Fig. 13. Effect of connectivity on runtime.

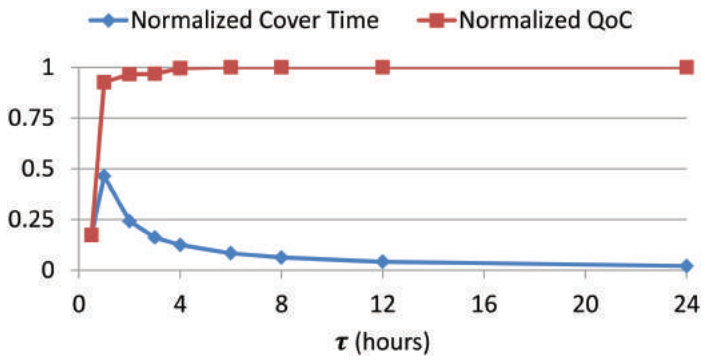

Fig. 14. Sampling interval vs. QoC.

interval is varied between 30 minutes and 24 hours. δ was varied to ensure that the energy used to sense per interval was the same for various sampling intervals.

Figure 14 shows the result. As expected, the QoC increases with the sampling interval. This is because increasing the sampling interval reduces the energy demand for the act of sensing and, as a result, allocates more harvested solar energy to battery charging. Ultimately this provides sensors with the ability to use larger radii to enhance the QoC.

The experiment was then repeated with δ as the parameter of interest. δ was varied between 1% and 100% of the 30-minute sampling interval. Figure 15 shows the result. It is evident that as δ increases, the QoC decreases due to the increased amount of energy required to sense a distance r. This decrease is more linear, unlike in the case of τ.

However, it is also important to note that by increasing τ and decreasing δ (i.e., increasing time between samples) we introduce periods in which the network is not being monitored at all. These periods mark points of vulnerability in many networks such as surveillance networks. To visualize this we slightly modify to the definition of cover to be the number of targets covered averaged over the operation time. This means that the points of zero cover due to the low value of δ (or high value of τ) impact the overall QoC. This new metric is shown in Figures 15 by the blue diamond-marked line. It is interesting to note that there exists a unique sampling interval that maximizes this new metric.

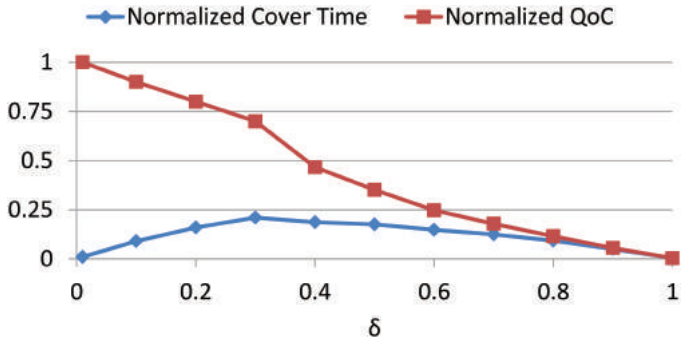

Fig. 15. δ vs. QoC.

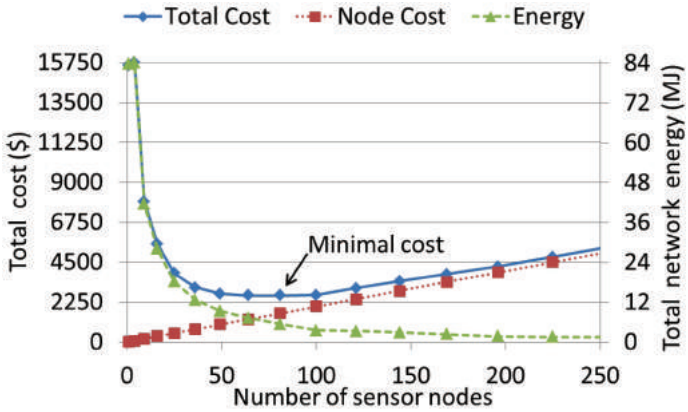

Fig. 16. Effect of number of sensor nodes on the network setup cost.

6.8. Effect of Number of Sensors on Network Setup Cost

In this experiment, we study the effect of the number of sensors on the total cost of setting up a sensor network to maintain a specified QoC. The results from this experiment offer network designers the information to trade off the number of sensors to minimize the initial setup cost of a sensor network. This is also useful to maintain an energy-neutral operation [Kansal et al. 2007], which implies minimum sizing of the battery and the solar panel to reduce the operation cost while guaranteeing a QoC for a given network.

For this experiment, a large number of targets (1024) are distributed over a 200 m $\times$ 200 m area in the same fashion as in Section 6.7. The requirement is that 100% of the targets must be covered. To calculate the network setup cost, we assume that each sensor node costs \$20 [Node Cost 2011], solar panel costs \$2/Watt [Sun Electronics 2011], and the batteries cost \$0.47/Watt-hour [Bat 2011]. With the assumption of 10 hours of sunlight per day, the results shown in Figure 16 are obtained.

Contradicting intuition, increasing the number of sensor nodes does not increase the total network energy. This is because, with more sensors, smaller radii can be used to achieve the same coverage, and the energy cost decreases at least quadratically with the radius. Because of the lower total network energy requirement, smaller batteries and solar panels are sufficient to maintain the original specified cover, thus decreasing the total network setup cost. However, an increase in the number of sensor nodes adds to the total setup cost. Thus, there exists a unique configuration of the number of

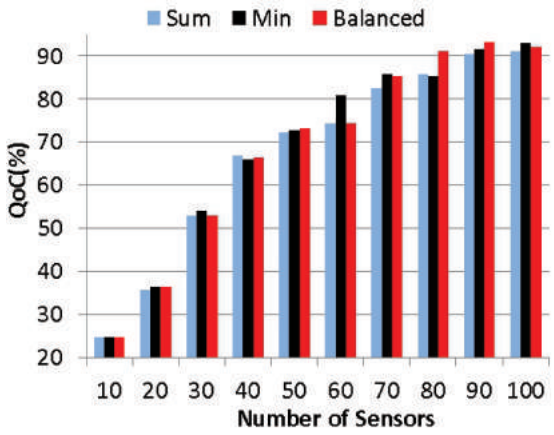

Fig. 17. Effect of various objective functions on QoC.

sensor nodes that minimizes the overall setup cost. This is shown in Figure 16. The plot shows a sharp initial reduction in the network energy as N increases, due to the nonlinear relation between the network energy and the sensor radii, and the fact that the effective sensor radii decrease quadratically with the increase in the number of nodes.

6.9. Investigation of Objective Functions

This experiment briefly examines the different possible objective functions that can be chosen for the quasiconvex problem in Eq. (19). As mentioned earlier in Section 5.1, the objective function in the reformulation of the problem can be considered as a dummy function. As such, we may consider other possible objectives. The first objective (35) is simply to minimize the overall energy consumed by the network, or equivalently, maximizing the total residual battery life of the network. The second objective (36) is to maximize the minimum residual battery among all nodes in the network. The third objective (37) offers a balance between the preceding two objectives. The same parameters from Section 6.6 are used. Results are shown in Figure 17.

$$\max_{\mathbf{r}(k),\boldsymbol{\chi}(k)} \quad \sum_{n\in S} e_{bat,n}(k). \qquad \text{(Sum)} \qquad (35)$$

$$\max_{\mathbf{r}(k),\boldsymbol{\chi}(k)} \quad \min_{n\in S} e_{bat,n}(k). \qquad \text{(Min)} \qquad (36)$$

$$\max_{\mathbf{r}(k),\boldsymbol{\chi}(k)} \quad \frac{1}{N}\sum_{n\in S} e_{bat,n}(k) + \min_{n\in S} e_{bat,n}(k). \qquad \text{(Balanced)} \qquad (37)$$

From the figure, it can be observed that no one objective function is consistently better than the other, over all values of N. However, the efficiency of solution method presented in this article makes it possible to explore the design space, as shown in Section 6.8, and determine which objective is best for a given network.

6.10. Effect of Beamwidth on QoC

The final design exploration experiment investigates the effect of varying beamwidths ϕ on QoC. In this experiment, the beamwidth is varied between 0° and 360°. The power density is kept constant and the maximum power output is capped at 100 W. Targets are dispersed in a 21×21 grid across a 40000 m^2 area. Likewise, 25 sensors

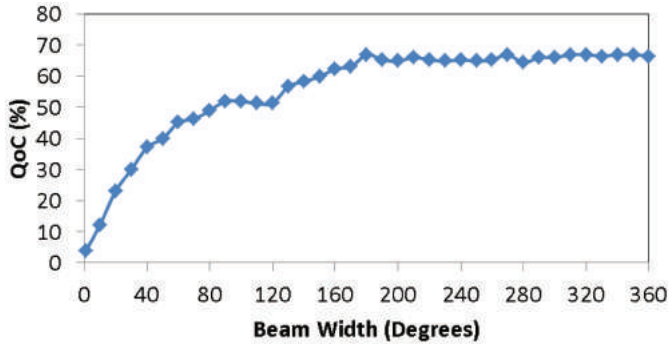

Fig. 18. Beamwidth vs. QoC.

are equally spaced in this region. All sensor beams face the same direction. The results are illustrated in Figure 18.

Despite the increase in power costs, increasing beamwidth almost always tends to increase the QoC (with few exceptions that may be attributed to the discrete nature of the cover model). That said, the rate at which QoC increases diminishes nonlinearly with beamwidth. In the aforesaid case, the maximum QOC of 67% is reached at a beamwidth of 180°. It should be noted that, oftentimes, omnidirectional sensors are constructed from a ring of narrow-beam sensors. For this reason, design costs could be decreased by creating only semi-directional sensors with no loss to QoC.

7. CONCLUSIONS

There has been a proliferation of energy-harvesting sensors in WSNs. The surge of "green" technology brings with it many additional challenges on optimal scheduling of sensor nodes to maximize the QoC. In this work, a novel, near-optimal solution is presented to the scheduling problem of active sensor nodes in the context of the target cover problem, which maximizes the minimum attainable QoC. The proposed quasiconvex solution not only considers the cover requirement, but also determines an efficient routing scheme to deliver all sensed data to the sink, which is often overlooked. The quasiconvex solution demonstrates a large speedup compared with the naive DP solution with a minimal error in accuracy.

The usefulness of the quasiconvex solution was extended by applying it to various design-space explorations of energy-harvesting sensor networks. The insights provided by these experiments lead to optimal sizing of sensor networks for minimum network startup cost. Furthermore, increasing beamwidth provides decreasing returns on QoC improvement. The experiments on varying sampling rates revealed that there is a unique sampling interval which maximizes the normalized QoC.

REFERENCES

I. F. Akyildiz, W. Su, Y. Sankarasubramaniam, and E. Cayirci. 2002. Wireless sensor networks: A survey. *Comput. Netw.* 38, 4, 393–422.

BAT. 2011. Battery energy: What battery provides more? http://www.allaboutbatteries.com/Battery-Energy.html.

S. Boyd and L. Vandenberghe. 2004. *Convex Optimization*. Cambridge University Press.

M. Cardei, J. Wu, M. Lu, and M. Pervaiz. 2005. Maximum network lifetime in wireless sensor networks with adjustable sensing ranges. In *Proceedings of the International Conference on Wireless and Mobile Computing, Networking and Communications (WiMob'05),* vol. 3. 438–445.

V. Chvatal. 1975. A combinatorial theorem in plane geometry. *J. Combin. Theory B18*, 1, 39–41.

S. Dasika, S. Vrudhula, and K. Chopra. 2006. Algorithms for optimizing lifetime of battery powered wireless sensor networks. In *Sensor Network Operations,* IEEE Press.

D. Diamond, S. Coyle, S. Scarmagnani, and J. Hayes. 2008. Wireless sensor networks and chemo-/biosensing. *Chem. Rev.* 108, 2, 652–679.

ELVA-1. 2012. 26.5ghz and 140ghz cassegrain antenna series for oem. http://www.elva-1.com/products/microwave/dual_reflect.html.

eZ4. 2009. eZ430-RF2500 development tool user's guide (rev. e). http://www.ti.com/lit/ug/slau227e/slau227e.pdf

H. Friis. 1946. A note on a simple transmission formula. *Proc. IRE* 34, 5, 254–256.

B. Gaudette, V. Hanumaiah, S. Vrudhula, and M. Krunz. 2012. Optimal range assignment in solar powered active wireless sensor networks. In *Proceedings of the International Conference on Computer Communications (Infocom'12).*

C.-F. Huang and Y.-C. Tseng. 2003. The coverage problem in a wireless sensor network. In *Proceedings of the 2nd ACM International Conference on Wireless Sensor Networks and Applications (WSNA'03).* ACM Press, New York, 115–121.

A. Kansal, J. Hsu, S. Zahedi, and M. B. Srivastava. 2007. Power management in energy harvesting sensor networks. *ACM Trans. Embed. Comput. Syst.* 6, 4.

D. Kirk. 1970. *Optimal Control Theory: An Introduction*. Prentice-Hall, Englewood Cliffs, NJ.

C. Liu, K. Wu, Y. Xiao, and B. Sun. 2006. Random coverage with guaranteed connectivity: Joint scheduling for wireless sensor networks. *IEEE Trans. Parallel Distrib. Syst.* 17, 562–575.

J. J. Michalsky. 1988. The astronomical almanac's algorithm for approximate solar position. *Solar Energy* 40, 227–235.

D. Niyato, E. Hossain, and A. Fallahi. 2007. Sleep and wakeup strategies in solar-powered wireless sensor/mesh networks: Performance analysis and optimization. *IEEE Trans. Mobile Comput.* 6, 221–236.

J. Nocedal and S. J. Wright. 2000. *Numerical Optimization*. Springer.

Node Cost. 2011. EZ430-rf2500t – msp430 2.4-ghz wireless target board. https://estore.ti.com/EZ430-RF2500T-MSP430-24-GHz-Wireless-Target-Board-P1295.aspx.

NREL. 2011. Solar resource and meteorological assessment project southwest solar solar cat, January 12, 2011 raw data. http://www.nrel.gov/biomass/publications.html.

NREL. 2000. Solar position calculator. http://www.nrel.gov/midc/solpos/.

J. O'Rourke. 1998. *Computational Geometry in C*. Cambridge University Press.

C. H. Papadimitriou and K. Steiglitz. 1982. *Combinatorial Optimization: Algorithms and Complexity*. Prentice-Hall, Upper Saddle River, NJ.

D. Rakhmatov and S. Vrudhula. 2003. Energy management for battery-powered embedded systems. *ACM Trans. Embed. Comput. Syst.* 2, 3, 277–324.

D. Rakhmatov, S. Vrudhula, and D. Wallach. 2003. A model for battery lifetime analysis for organizing applications on a pocket computer. *IEEE Trans. VLSI Syst.* 11, 6, 1019–1030.

R. Rao, S. Vrudhula, and D. Rakhmatov. 2003. Battery modeling for energy-aware system design. *IEEE Comput.* 36, 12, 77–87.

M. Skolnik. 1962. *Introduction to Radar Systems*. McGraw-Hill.

Sun Electronics. 2011. http://www.sunelec.com/.

P. Torcellini, S. Pless, M. Deru, and D. Crawley. 2006. Zero energy buildings: A critical look at the definition. Presented at ACEEE Summer Study, National Renewable Energy Laboratory. http://www.nrel.gov/docs/fy06osti/39833.pdf.

T. Voigt, A. Dunkels, J. Alonso, H. Ritter, and J. Schiller. 2004. Solar-aware clustering in wireless sensor networks. *Comput. Comm.* 1, 238–243.

A. Wang, S. Cho, C. Sodini, and A. Chandrakasan. 2001. Energy efficient modulation and mac for asymmetric rf microsensor systems. In *Proceedings of the International Symposium on Low Power Electronics and Design (ISLPED'01).* ACM Press, New York, 106–111.

J. Yick, B. Mukherjee, and D. Ghosal. 2008.Wireless sensor network survey. *Comput. Netw.* 52, 2292–2330.

O. Younis, S. Ramasubramanian, and M. Krunz. 2007. Operational range assignment in sensor and actor networks. *Ad Hoc Wirel. Netw.* 5, 1–2, 1–37.

H. Zhang and J. Hou. 2004. Maintaining sensing coverage and connectivity in large sensor networks. *Ad Hoc Wirel. Peer-to-Peer Netw.* 1, 89–124.

Received October 2012; revised July 2013; accepted August 2013